CELL BIOLOGY

An in vivo screen identifies diverse domains that can act as force-dependent proteolytic switches for Notch activation

Frederick C. Baker[1], Jacob Harman[1], Trevor Jordan[1], Breana Walton[1], Amber Ajamu-Johnson[1], Rama F. Alashqar[1], Simran Bhikot[1], Gary Struhl[2,3], Paul D. Langridge[1]*

Notch proteins are single-pass transmembrane receptors activated by sequential extracellular and intramembrane cleavages to release the cytosolic domains that function as transcription factors. Transmembrane ligands of the Delta/Serrate/LAG-2 (DSL) family activate Notch on neighboring cells by exerting a pulling force across the intercellular ligand-receptor bridge. This force is generated by Epsin-mediated endocytosis of the ligand into the signal-sending cell and results in the extracellular cleavage of the force-sensing negative regulatory region (NRR) of the receptor by an ADAM10 protease on the signal-receiving cell. Here, we used chimeric Notch and DSL proteins to screen for other domains that could function as ligand-dependent proteolytic switches in place of the NRR in the developing *Drosophila melanogaster* wing. The domains that could functionally substitute for the NRR in vivo derived from diverse source proteins, varied in sequence, and had different predicted structures, yet all depended on cleavage that was catalyzed by the *Drosophila* ADAM10 homolog Kuzbanian (Kuz) and stimulated by Epsin-mediated ligand endocytosis. The large sequence space of protein domains that can serve as force-sensing proteolytic switches suggests a widespread potential role for force-dependent, ADAM10-mediated proteolysis in other cell contact–dependent signaling mechanisms.

INTRODUCTION

Many processes in biology depend on contact-dependent, juxtacrine signaling in which transmembrane ligands and receptors form intercellular bridges between ligand-bearing sending cells and receptor-bearing receiving cells. Such bridges are likely exposed to pulling forces as one or both ends of the bridge undergo endocytosis, and the resulting mechanical tension across the bridge can lead to ectodomain cleavages that regulate signaling. A prototypical example is the receptor Notch, a highly conserved single-pass transmembrane protein that has profound and pervasive roles in development, physiology, and disease (*1*–*3*). Notch is activated by single-pass transmembrane ligands of the conserved Delta/Serrate/LAG-2 (DSL) family. Upon binding to Notch, DSL ligands induce cleavage and shedding of the Notch ectodomain by an ADAM10 (a disintegrin and metalloproteinase 10) protease, the *Drosophila melanogaster* homolog of which is Kuzbanian (Kuz), tethered to the surface of the receiving cell (*4*–*6*). Ectodomain shedding renders the rest of the receptor a substrate for intramembrane cleavage by γ-secretase (*7*–*9*), releasing the Notch cytoplasmic domain (NICD)—a transcription factor—for entry into the nucleus (*10*–*13*).

For Notch, activation depends on mechanical tension exerted across the intercellular ligand-receptor bridge by endocytosis of the ligand into the sending cell. Specifically, upon binding to Notch, DSL ligands are recruited to the Clathrin-dependent endocytic pathway by the adapter protein Epsin (*14*–*16*). The process of ligand recruitment and/or internalization then generates a pulling force across the ligand-receptor bridge that renders it susceptible to ADAM10-mediated proteolysis (*17*, *18*). Both in vivo and biophysical studies indicate that cleavage depends on the exposure of an otherwise buried site in a conserved juxtamembrane negative regulatory region (NRR) that behaves as a force-sensitive proteolytic switch (*17*, *19*). The key role of the NRR can be recapitulated using a heterologous force-dependent proteolytic switch—the A2 domain of Von Willebrand factor (*20*, *21*)—in place of the NRR, provided that it is tuned to the appropriate force (*18*).

The ectodomains of many other cell surface proteins are also cleaved by ADAM10 proteases (*22*, *23*), raising the possibility that force-dependent, ADAM10-mediated proteolysis plays a more general role in juxtacrine signaling. In support, although many ADAM10 substrate proteins are cleaved constitutively [for example, (*24*)], proteolysis of at least some receptor substrates depends on the receptor binding to its cognate ligand (*5*, *25*). However, the sheer number of ADAM10 substrates identified to date [at least 100 (*26*)] and the lack of a defined consensus cleavage site (*27*) make it difficult to assess the prevalence of ADAM10-dependent, force-sensitive switches in juxtacrine signaling. Moreover, the possibility that any given ADAM10-sensitive domain functions as a proteolytic switch needs to be validated experimentally. Such tests have yielded positive results in a cell culture screen that included sea urchin enterokinase agrin–like (SEA) domains, which have structural similarity with Notch NRRs and are found in many transmembrane receptors and other cell surface proteins (*28*). The capacity of SEA domains to function as NRR-like proteolytic switches in cell culture is consistent with a more general role for such domains in force-sensitive signaling events. However, it is unclear how well cell culture conditions capture the native signaling processes in vivo, where the relevant interactions often occur between cells in polarized epithelia, and for which ligand and/or receptor endocytosis may be necessary to generate the requisite, activating force. Also unclear is the structural diversity of domains that have the potential to act as ADAM10-dependent proteolytic switches.

[1]Department of Biological Sciences, Augusta University, Augusta, GA 30912, USA. [2]Department of Genetics and Development, Vagelos College of Physicians and Surgeons, Columbia University, New York, NY 10027 USA. [3]Mortimer B. Zuckerman Mind Brain Behavior Institute, New York, NY 10027, USA.
*Corresponding author. Email: plangridge@augusta.edu

Here, we present the results of an in vivo screen designed to identify protein domains that can function as proteolytic switches in place of the Notch NRR. The screen was predicated on the use of chimeric forms of *Drosophila* Notch and Delta in which the native ligand and receptor ectodomains were replaced by heterologous ligand and receptor binding domains, and productive signaling was monitored in vivo by the induction of Notch target genes in wing imaginal discs (*18*). Of 43 tested chimeric Notch receptors that contained different candidate switch domains, we identified 11 that responded to ligand in an Epsin- and Kuz-dependent manner. These proteolytic switches derive from a wide range of proteins and appear diverse in structure, indicating that the repertoire of possible switch domains is large and suggesting that many different cell surface proteins have the potential to be force-dependent targets for Kuz or other ADAM10 proteases. Our results also validate the screen as a means to identify new switch domains that can be used to diversify the collection of available synthetic Notch (synNotch) receptors for biomedical applications (*29*, *30*).

RESULTS

In vivo screen for putative force-sensitive proteolytic switches that can substitute for the Notch NRR

To screen protein sequences for their capacity to function as NRR-like proteolytic switches, we generated transgenes that encode chimeric Notch receptors in which (i) the ligand-binding, epidermal growth factor (EGF) repeat domain of the native receptor was replaced by the ligand-binding domain of the follicle stimulating hormone receptor (FSHR), and (ii) the juxtamembrane NRR was replaced by candidate switch domains from other proteins (Fig. 1, A and B). All such FSHR-Notch chimeric receptors retain the transmembrane and intracellular domains of the native Notch receptor that drive well-characterized transcriptional and morphological outputs of the Notch signaling pathway (*18*). We then asked whether each of these receptors can be activated in vivo by a chimeric form of Delta (Dl) in which the ectodomain is replaced by follicle-stimulating hormone (FSH-Dl). Native FSH is a heterodimer of distinct α and β subunits. As in our prior studies (*18*, *31*), we generated the functional FSH-Dl ligand by coexpressing an otherwise inactive FSHβ-Dl ligand together with secreted FSHα. Because virtually all of our experiments were performed in the presence of coexpressed FSHα, we refer to the FSHβ-Dl coding sequence and encoded protein—for convenience—as FSH-Dl, except when we perform negative controls in which it is expressed in the absence of FSHα.

To execute this approach at scale, we incorporated three strategies to optimize generating chimeric FSHR-Notch receptors and testing their capacity to respond to FSH-Dl. First, the coding sequences for a collection of FSHR-Notch chimeric receptors, each having a different protein domain in place of the native NRR, were introduced into a series of transformation vectors. These were bar-coded by using

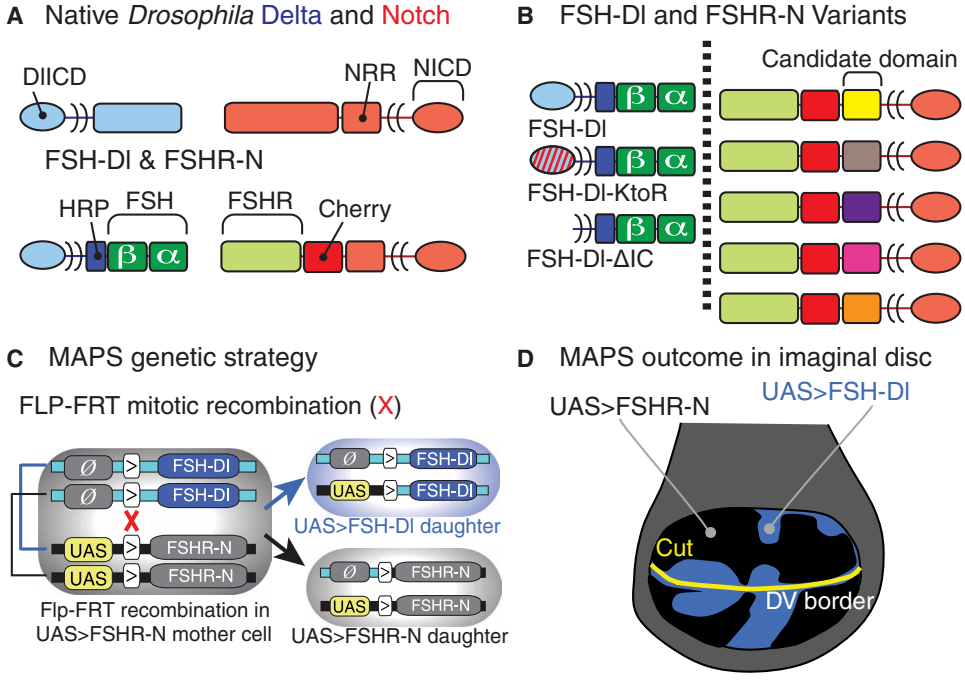

Fig. 1. Functional screen to identify force-sensitive cleavage domains in vivo. (**A**) Cartoons show the domain structures of *Drosophila* Delta (Dl) and Notch (N) and the FSH-Dl and FSHR-N chimeras in which the ligand-binding regions of Dl and N were replaced with functional heterologous binding regions, and HRP and Cherry tags were inserted as indicated. The Dl extracellular domain was replaced by FSHβ, and coexpression of FSHα reconstitutes the composite FSH ligand. Reciprocally, the ligand-binding portion of the N ectodomain was replaced by the FSHR ectodomain. The intracellular domains of N (NICD) and Dl (DllCD) were not altered. (**B**) FSHR-N receptor was modified by replacing the NRR of Notch with a single candidate sequence to produce 43 different FSHR-N receptors, each with distinct juxtamembrane regions. FSH-Dl was used for the screen but modified for subsequent analyses by replacing DllCD, which targets FSH-Dl for Epsin-dependent endocytosis, with domains that exclude the ligand from that route, either through mutation of each of the lysines in the intracellular domain to arginine (FSH-Dl-KtoR) or by removal of the intracellular domain entirely (FSH-Dl-ΔIC). (**C**) MAPS allows the generation of interfaces between clones of FSH-Dl–expressing cells and surrounding FSHR-N–expressing tissue. The coding sequences of the chimeric FSHR-N receptors were placed downstream of a UAS promoter controlled by the yeast Gal4 transcription factor but separated from the promoter by a target for mitotic recombination catalyzed by the yeast Flp recombinase (FRT, indicated as >). All of the resulting *UAS>FSHR-N* transgenes were inserted at the same attP genomic docking site (cytological position 86Fb) and in the same orientation as a *Ø>FSH-Dl* transgene that lacks a functional promoter (Ø). Consequently, transheterozygous *UAS>FSHR-N/Ø>FSH-Dl* cells express only FSHR-N in response to Gal4. However, when subjected to heat shock–induced Flp recombinase, these cells can undergo mitotic recombination across the FRTs (red X) to generate single cells in which the *UAS* promoter drives expression of the ligand rather than the receptor. Only one of the two possible segregation outcomes is shown (indicated by brackets); the alternative segregation event also results in an FSH-Dl–expressing daughter cell adjacent to sibling and parental cells that express only FSHR-N. (**D**) MAPS-generated *UAS>FSH-Dl* founder cells develop to form clones surrounded by *UAS>FSHR-N* tissue in the wing pouch of the imaginal disc. The prospective wing includes cells expressing either FSH-Dl, which can be detected by the HRP epitope tag (blue), or FSHR-N under Gal4/UAS control (black). Peak amounts of native DSL-N signaling induce the expression of the N target gene *cut* along the boundary between the dorsal (D) and ventral (V) compartments (Cut protein, yellow).

different transgenic markers, including variously deleted forms of a genomic *yellow*$^{+}$ rescuing fragment that generate different patterns of body and bristle pigmentation in a *yellow* mutant background. This allowed us to microinject mixtures of several transgenes in a single microinjection and then to distinguish transformants of each transgene by phenotype, thus saving time, materials, and cost.

Second, we used transformation vectors designed to be compatible with our mosaic analysis by promoter swap (MAPS) technique (*18*). The coding sequence for each receptor was placed downstream of an upstream activating sequence (UAS) promoter followed by an FRT (>) recombination target sequence to form the *UAS>FSHR-Notch* transgenes. Each *UAS>FSHR-Notch* transgene was introduced at the 86Fb genomic docking site. The FSH-Dl coding sequence was placed downstream of an FRT, but with no promoter (Ø), to form *Ø>FSH-Dl*, and inserted at the 86Fb genomic docking site. Consequently, transheterozygous *UAS>FSHR-Notch/Ø>FSH-Dl* cells express only FSHR-Notch in response to Gal4. However, when subjected to heat shock–induced Flp recombinase, these cells can undergo mitotic recombination across the FRTs to generate cells in which the *UAS* promoter now drives expression of the ligand rather than the receptor. This allowed us to generate potential signaling interfaces between clones of FSH-Dl–expressing cells and surrounding FSHR-Notch–expressing tissue [described in detail in Fig. 1C and (*18*)].

Third, we used a *nubbin.Gal4* (*nub.Gal4*) transgene to drive expression of *UAS>FSH-Dl* and *UAS>FSHR-Notch* transgenes in the pouch of the wing imaginal disc—a circular domain within the disc destined to form the adult wing (Fig. 1D). Normally, peak DSL-Notch signaling in the pouch is restricted to a thin stripe of cells flanking the dorsoventral (DV) boundary, where it induces expression of the transcription factor Cut, specifies formation of wing margin bristles, and directs local production of Wingless (Wg), a morphogen that controls wing growth (*32*–*34*). Early heat shock induction of *UAS>FSH-Dl* clones in *UAS>FSHR-Notch* wing discs generates clonal interfaces between dedicated FSH-Dl– and FSHR-Notch–expressing cells. If a given FSHR-Notch receptor can be activated by FSH-Dl, then these interfaces will induce ectopic expression of Notch target genes and altered wing morphology, both of which are easy to score in vivo.

Candidate domains for NRR-like proteolytic switches

We chose to test domains from a diverse collection of proteins to assess the efficacy of the screen and the repertoire of structures that can mediate Notch cleavage in response to force (Table 1). Kuz/ADAM10 proteolysis typically targets the juxtamembrane extracellular regions of cell surface proteins, and the amino acid sequence cleaved varies among substrates. Hence, we mostly tested domains positioned immediately N-terminal to the transmembrane domain of cell surface proteins involved in juxtacrine signaling and did not restrict the choice to domains with particular structural features. We also included several miscellaneous peptide sequences and protein domains. Candidate domains differed in length and structural composition, including juxtamembrane regions from surface receptors [for example, Ephrin receptors (Eph)], proteolytic switches previously identified in cell culture [table S1 and (*28*)], unstructured domains (for example, Flagelliform, a spider silk protein that is a concatemer of glycine-proline-alanine repeats), protein domains suggested by serendipitous findings (for example, Venus fluorescent protein), and truncated versions of the native Notch NRR. Last, for benchmarks, we used the intact NRRs of *Drosophila* Notch (NRR^{Notch}) and the *Caenorhabditis elegans* Notch homolog LIN-12 (NRR$^{LIN\text{-}12}$), which we have characterized in previous work (*18*, *31*). Both are strictly ligand dependent, but NRR^{Notch} is tuned to a force threshold requiring the pulling from Epsin, whereas NRR$^{LIN\text{-}12}$ is tuned to a lower threshold that does not. We present, below, the results of a screen of 43 *UAS>FSHR-Notch* transgenes, each encoding a different candidate proteolytic switch domain.

Assaying candidate proteolytic switches by adult wing phenotype and Notch target gene expression

To test the capacity of the different FSHR-Notch chimeric receptors to respond to FSH-Dl, females carrying each transgene were outcrossed to tester males carrying the *nub.Gal4*, *UAS.FSHα*, *hsp70.flp*, and *Ø>FSHβ-Dl* transgenes. Their progeny were then heat shocked early in larval life to induce expression of the *hsp70.flp* transgene and generate *UAS>FSH-Dl* clones in *UAS>FSHR-Notch* wing discs, and the resulting progeny were screened for abnormal wing phenotypes indicating ectopic FSHR-Notch activity (Fig. 2A).

UAS>FSHR-Notch transgenes that scored positively in the wing assay encode FSHR-Notch receptors that were either activated by ligand or constitutively active. These two possibilities were distinguished in the test cross of *UAS>FSHR-Notch* females to *UAS.FSHα; Ø>FSHβ-Dl* males because only female progeny coexpress FSHα, which is required for ligand activity, whereas male progeny do not (Fig. 2A). Accordingly, *UAS>FSHR-Notch* transgenes that caused abnormal wings in both male and female progeny encoded constitutively active receptors, whereas those that did so only in female progeny encoded receptors that were activated by ligand.

To corroborate and extend our classification of FSHR-Notch receptors that scored positively based on the initial wing assay, we repeated the MAPS experiments, this time analyzing the expression of the Notch target gene, *cut*, as monitored by staining for Cut protein, in the developing wing imaginal disc. Cut expression in the wing primordium is normally restricted to a thin strip of cells along the DV compartment boundary in response to peak Notch activation (Fig. 1D). Hence, both ligand-dependent and constitutively active FSHR-Notch receptors should cause ectopic Cut expression, whereas receptors that are refractory to activation should not. By design, the canonical FSH-Dl and FSHR-Notch proteins are epitope-tagged, respectively, with horseradish peroxidase (HRP) and Cherry fluorescent protein (Fig. 1A). As a consequence, both *UAS>FSH-Dl* clones and the surrounding *UAS>FSHR-Notch* tissue were identified with single-cell resolution by monitoring HRP and/or Cherry expression, allowing inductive signaling and constitutive activity to be assayed by monitoring for ectopic Cut expression at or away from the clone borders.

Of the 43 *UAS>FSHR-Notch* transgenes tested, most (40 of 43) fell into one of three distinct categories on the basis of both Cut expression in the wing imaginal disc (Fig. 2B) and the adult wing phenotype (Table 1 and table S2): 8 of 43 showed ectopic Cut restricted to FSHR-Notch–expressing cells located near or next to FSH-Dl–expressing cells, indicating ligand-dependent activation; 12 of 43 showed ectopic Cut in FSHR-Notch–expressing cells regardless of the presence of FSH-Dl–expressing cells, indicative of constitutive activation; 20 of 43 receptors showed no ectopic Cut expression, indicating the encoded receptors were refractory to activation. However, the remaining 3 of 43 transgenes were exceptional in encoding receptors that showed evidence of both constitutive activity and the capacity to respond to ligand, as described below. Hence, they fell into to a special class of "hyperactive" receptors,

Table 1. Domains that mediated ligand-dependent and constitutive activation of chimeric FSHR-Notch receptors. Columns describe the domain's activation class, abbreviated name, the identity of the native source protein and species, the size of the domain (#AA = number of amino acids), a brief description of the native source protein and the reason for its inclusion in the screen. Candidate domains cleaved in response to ligand are categorized as class I (high force tuning), class II (low force tuning), and class III ("hyperactive"). See also table S1 for comparison to the SNAPS (Synthetic Notch Assay for Proteolytic Switches) cell culture assay (*28*) that previously tested domains for proteolytic switch behavior. See table S2 for a complete list of all tested candidate domains. GFP, green fluorescent protein; ICD, intracellular domain.

Activation class	Name	Domain source	Species	Size (#AA)	Description	Reason for inclusion in screen
Ligand dependent class I	DCC	Deleted in colorectal cancer/Frazzled	*Drosophila*	18	Neuronal guidance receptor	Evidence that ICD acts as a transcription factor
	EphB2	EphB2 receptor	Mouse	110	Neuronal guidance receptor	Native receptor is cleaved in response to ligand binding
	DEph	Eph receptor	*Drosophila*	250	Neuronal guidance receptor	Native receptor is cleaved in response to ligand binding
	Serrate	Serrate	*Drosophila*	264	Notch ligand	Cleaved by Kuz
	FAT1	FAT1	Human	93	Atypical cadherin	SNAPS result: Cleavage in response to ligand
Ligand dependent class II	Dscam1	Down syndrome cell adhesion molecule 1	*Drosophila*	220	Neuronal guidance protein	Evidence that ICD acts as a transcription factor
	VenusGFP	Venus GFP	*Aequorea victoria*	242	Entire coding region of Venus GFP	Serendipitous result
	DAG1	Dystroglycan	Human	261	Cell adhesion and ECM-binding protein	SNAPS result: Cleavage in response to ligand
Ligand dependent class III	NRRΔLNR	Notch variant	*Drosophila*	45	Variant of the NRR of Notch	LNRs removed, but S2 site remains
	EPHRINB1	EPHRINB1 ligand	Human	74	Neuronal guidance protein	Native ligand is cleaved in response to ligand binding
	Flagelliform	Flagelliform F40	Spider	44	Spider silk–40 PGGAG repeats	Biophysically demonstrated to stretch at piconewton forces
Constitutive	DEphrinB	EphrinB ligand	*Drosophila*	74	Neuronal guidance protein	Native ligand is cleaved in response to ligand binding
	Robo	Roundabout 1	*Drosophila*	371	Neuronal guidance receptor	DCC/Frazzled related protein
	Neogenin	Neogenin	Mouse	367	Neuronal guidance receptor	ADAM10 substrate
	EphrinB2L	EphrinB2 (long)	Mouse	342	Neuronal guidance protein, includes juxtamembrane region, and two fibronectin domains	Cleavage in response to receptor binding
	EphrinB2S	EphrinB2 (short)	Mouse	110	Neuronal guidance protein, includes juxtamembrane region	Cleavage in response to receptor binding
	EPHB1	EPHB1 receptor	Human	124	Neuronal guidance receptor	Receptor cleavage in response to ligand binding
	Delta	Delta	*Drosophila*	34	Notch ligand	Cleaved by Kuz
	APP	Amyloid-beta precursor protein	Human	240	Neuronal repair protein	ADAM10 substrate
	CD16	CD16	Human	194	Immune cell receptor	ADAM10 substrate
	CD44	CD44	Mouse	461	Cell adhesion glycoprotein	ADAM10 substrate
	CDHR2	Cadherin-related family member 2	Human	356	Cell adhesion protein	SNAPS result: Cleavage in response to ligand
	E-cad	Epithelial cadherin	Mouse	161	Cell adhesion protein	ADAM10 substrate

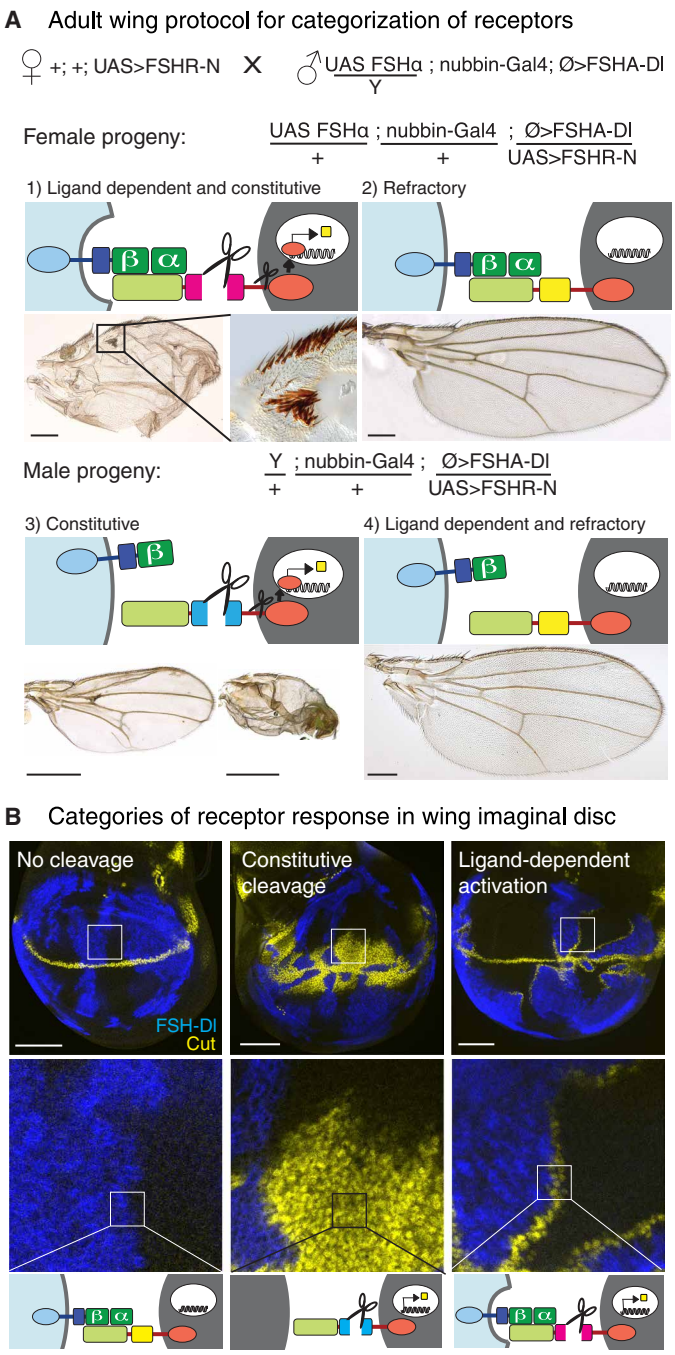

Fig. 2. Identification of categories of receptor activation. (**A**) To screen for receptor activation, G1 female flies carrying *UAS>FSHR-N* were crossed with male flies from a ligand tester stock carrying components for both UAS and Gal4 expression in the wing and the FSH-Dl ligand: *UAS.FSHα* on the X chromosome and the *nub.Gal4* driver and the *Ø>FSHβ-Dl* transgene on autosomes. FSH-Dl/FSHR-N interfaces were induced by MAPS, and receptor activation was categorized into four types by examining adult wing phenotypes resulting from the ectopic activation of Notch target genes. In female progeny, ligand-dependent and constitutive FSHR-N activation leads to ectopic wing margin and smaller wings (a ligand-dependent interaction is shown), but a receptor that is refractory to cleavage produces wild-type wings. Male progeny do not express functional FSH-Dl because they do not inherit the X chromosome carrying the *UAS.FSHα* transgene. If the FSHR-N variant is constitutively active, receptor activation can occur even in the absence of the *UAS.FSHα* transgene, resulting in an abnormal wing phenotype that varies according to the extent of receptor activation and the random positioning of the receptor clones. Examples of phenotypes resulting from low (left) and high (right) receptor activation are shown, with the major phenotype being a reduction in size, change in wing shape, and ectopic wing margin. If the FSHR-N variant is refractory to cleavage or undergoes only ligand-dependent cleavage, a wild-type wing results. Images are representative of $n = 20$ to 30 wings per FSHR-N variant. Scale bars, 200 μm. (**B**) Patterns of receptor activation in the wing imaginal disc were divided into one of three main categories. If the candidate domain is not cleaved, then clones of FSH-Dl (HRP^+, blue) do not produce ectopic Cut at the interface with FSHR-N cells (HRP^-, black), and native Cut (yellow) remains at the DV boundary. Constitutive cleavage allows FSHR-N activation regardless of the presence of ligand, resulting in ectopic Cut produced in all FSHR-N cells, including in those far from FSH-Dl cells. Ligand-dependent cleavage of FSHR-N induces ectopic Cut only in FSHR-N cells adjacent to FSH-Dl cells. Scale bars, 50 μm. Images are representative of $n = 4$ to 23 wing discs for each FSHR-N variant.

increasing the number we designated as ligand dependent from 8 of 43 to 11 of 43 (Table 1).

UAS>FSHR-Notch transgenes that scored negatively encode receptors that are refractory to activation by ligand, consistent with the candidate domain not being able to function as a proteolytic switch. However, a bona fide force sensor might nevertheless score negatively for a number of reasons. These include the following: (i) It is tuned to a sufficiently high force threshold such that it cannot be activated by FSH-Dl [for example, as is the case for the native A2 domain from von Willebrand factor (VWF) (*18*)]; (ii) cleavage occurs at a site positioned sufficiently far away from the receptor transmembrane domain to preclude cleavage by γ-secretase, which depends on the size of the remaining ectodomain stub (*9*); or (iii) the candidate domain being tested is inadvertently truncated or impaired by adventitious interactions with neighboring protein sequences to render it inoperable as a switch domain. Hence, we drew no conclusions about the receptors encoded by *UAS>FSHR-Notch* transgenes that tested negatively but, instead, focused our analysis exclusively on the *UAS>FSHR-Notch* transgenes that yielded positive results.

Reliance of ligand-dependent FSHR-Notch receptors on Epsin-mediated ligand endocytosis

Given our prior evidence that cleavage of the native NRR depends on the force generated by Epsin-mediated ligand endocytosis (*18*), we next asked whether activation of the 11 ligand-dependent FSHR-Notch receptors depended on Epsin. Signaling by DSL ligands normally depends on ubiquitylation of cytosolic lysine residues for recruitment to the Clathrin-dependent endocytic pathway by Epsin (*15*, *16*). Hence, native DSL ligands in which all lysines in the cytosolic domain are replaced by arginine (KtoR forms) have greatly reduced capacity to enter the Epsin pathway, whereas those that lack a cytosolic domain are entirely unable to do so (*18*, *35*, *36*). In the context of FSH-Dl/FSHR-Notch signaling in the wing disc, the NRR^{Notch} and $NRR^{LIN\text{-}12}$ benchmark receptors appear to define opposite ends of an Epsin-dependent force spectrum. Both the FSH-Dl-KtoR and FSH-Dl-ΔIC ligands fail to induce detectable activation of the FSHR-Notch receptor with NRR^{Notch} (*18*), whereas both are similarly effective as the wild-type FSH-Dl ligand in activating the $NRR^{LIN\text{-}12}$ receptor (*31*). We interpret this difference as due to the $NRR^{LIN\text{-}12}$ having a lower force threshold for cleavage than NRR^{Notch}. Accordingly, we used the capacity of the 11 ligand-dependent FSHR-Notch receptors to respond to wild-type, KtoR, and ΔIC forms of FSH-Dl to assess the force sensitivity of their candidate proteolytic switch domains.

To perform this comparison, we took advantage of our previous finding that the distance from the DV boundary that FSH-Dl/FSHR-Notch signaling can induce ectopic Cut expression provides an indication of the strength of signaling (*18*). To normalize for variations in wing disc size, this measurement is expressed as the ratio of the maximum distance of ectopic Cut expression from the DV boundary relative to the length of the DV border. Previously, we used this assay to provide evidence that the benchmark NRR^{Notch} and $NRR^{LIN\text{-}12}$ receptors are tuned to different force thresholds [Fig. 3A and (*18*, *31*)]. Using this approach, we found that the 11 candidate proteolytic switch domains fell into three distinct classes of force sensitivity.

Class I receptors (5 of 11) behaved similarly to receptors containing the native Notch NRR. These chimeric receptors contained protein domains from the receptors deleted in colorectal cancer (DCC), Ephrin type-B receptor 2 (EphB2) and *Drosophila* Eph (DEph), the *Drosophila* DSL ligand Serrate, and the human protocadherin FAT1. Specifically, they showed a readily detectable response to FSH-Dl but little or no response to FSH-Dl-KtoR or FSH-Dl-ΔIC, indicating a strong—if not absolute— requirement for Epsin-dependent pulling (Fig. 3B). This is similar to what we have observed previously for both the native Notch NRR and disease-associated mutant forms of the A2 domain from VWF [such as $A2^{E1638K}$ (*18*)], consistent with all five of the newly identified class I domains being tuned to respond to force thresholds on par with that of the native Notch NRR.

Class II receptors (3 of 11) differed from class I receptors in showing a modest response to FSH-Dl-KtoR and weak or no response to FSH-Dl-ΔIC (Fig. 3C). Hence, these switches appear intermediate in their force tuning between the native *Drosophila* NRR^{Notch}, which is strictly Epsin dependent, and the *Caenorhabditis elegans* $NRR^{LIN\text{-}12}$, which appears to be Epsin independent [Fig. 3A and (*31*)]. These class II domains came from Venus fluorescent protein (Venus), Down syndrome cell adhesion molecule (Dscam1), and dystroglycan 1 (DAG1).

Class III receptors (3 of 11) are those we designate as hyperactive, showing both ligand-dependent and constitutive activity. They carry candidate switch domains from Flagelliform, EPHRINB1, and a partial deletion of the fly Notch NRR ($NRR^{\Delta LNR}$) that retains the native Kuz target site but removes the three conserved Lin-12 Notch repeats (LNRs) that normally occlude it. For these receptors, we found that Cut was present at peak amounts in FSHR-Notch–expressing cells near FSH-Dl– or FSH-Dl-KtoR–expressing cells but in lower amounts further away (Fig. 4A). In the absence of ligand, ectopic Cut expression was detected, but it was restricted to the vicinity of the DV boundary, where we infer that a low amount of constitutive activity of the FSHR-Notch receptor boosted the native response of endogenous Notch to Dl above a threshold necessary to generate detectable Cut expression (Fig. 4B). Hence, we interpret these class III hyperactive receptors as having low constitutive activity and a readily detectable response to ligand, and this forms a subcategory of the ligand-dependent receptors (Table 1).

It should be noted that FSHR-Notch receptors carrying different ligand-dependent switch domains showed a wide range of responses to FSH-Dl, as monitored by the distance over which Cut can be induced away from the DV boundary. However, we do not know where the different candidate domains are cleaved, which determines the susceptibility of the truncated receptor to Presenilin-dependent transmembrane cleavage (*9*). Further, the expression amount or surface distribution of different receptors may vary. Therefore, we do not draw any inferences about differences in force tuning on the basis of comparing the spatial responses of different FSHR-Notch receptors to FSH-Dl. Instead, we draw such inferences only from comparing the responses of the same FSHR-Notch receptor to FSH-Dl versus FSH-Dl-KtoR or FSH-Dl-ΔIC, which we interpret as indicating the relative reliance on Epsin-dependent endocytic force.

Candidate force-sensitive domains require the ADAM protease Kuzbanian for cleavage

The 11 force-sensitive candidate domains and the 12 domains that were constitutively cleaved have little common sequence similarity, including in the positioning of hydrophobic amino acids that in some substrates are preferentially found close to ADAM10 cleavage sites [(*27*) and fig. S1]. The candidate domains also have broad structural diversity based on AlphaFold predictions (fig. S2, A and

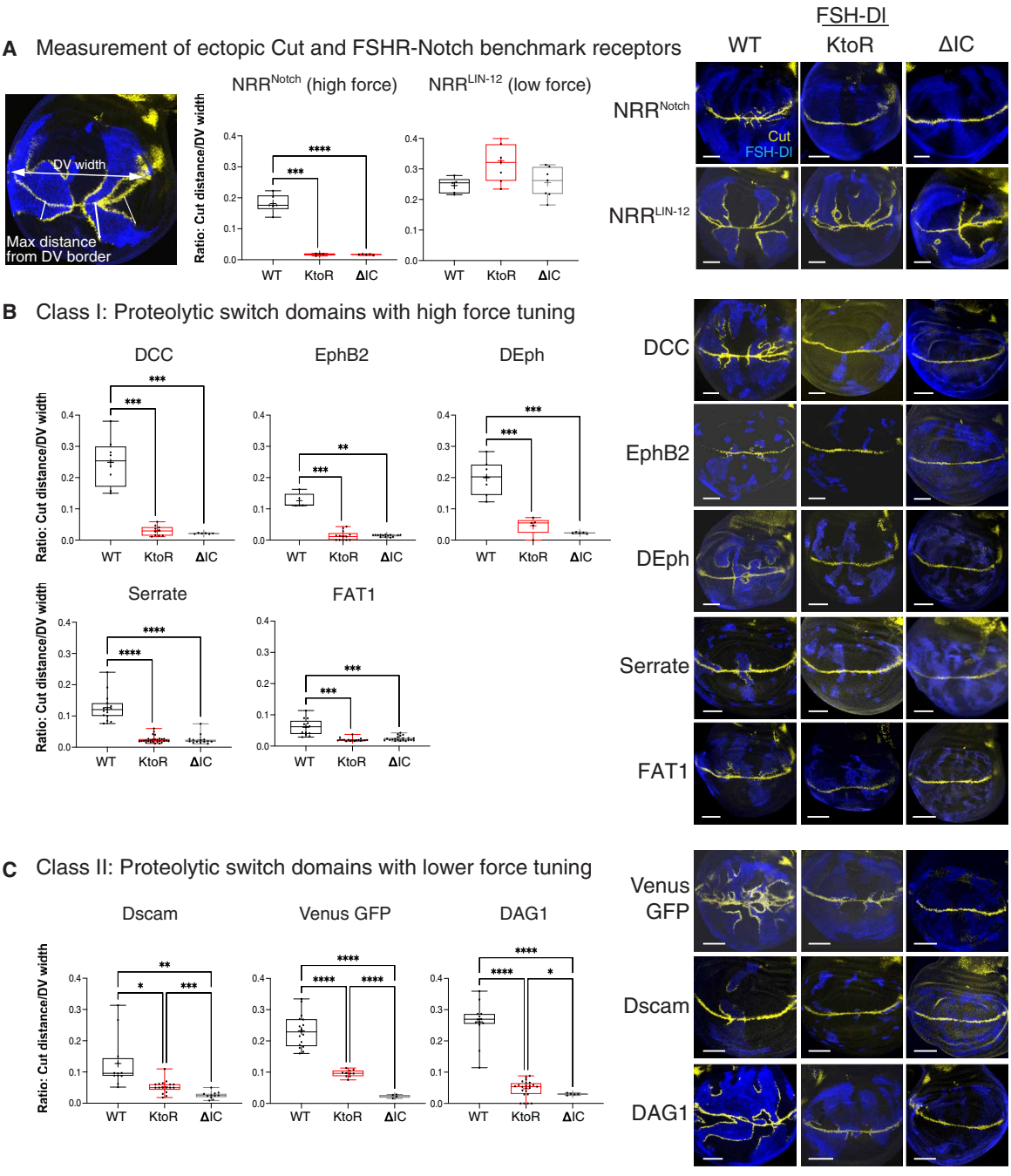

Fig. 3. Requirement for Epsin-mediated ligand endocytosis in receptors showing ligand-dependent activation. (**A**) Quantitation of signaling between cells expressing FSH-Dl (HRP^+, blue) and cells expressing FSHR-N variants containing domains cleaved in response to ligand (HRP^-, black). This was measured as the distance ectopic Cut (yellow) extended away from the DV boundary relative to disc size and is presented as a ratio of the two distances. Signal strength is depicted as boxplots that show the cut distance/DV width ratio for each disc as a point, as well as the mean (cross), median (horizontal line), and 25 to 75% interquartile ranges (tops and bottoms of the box) for each receptor-ligand combination. Each receptor was confronted with three different FSH-Dl variants with intracellular domains corresponding to the wild-type Dl domain (WT), the KtoR mutated Dl domain (KtoR), and a deletion of the intracellular domain (ΔIC). As benchmarks, the responses to FSH-Dl ligands of the FSHR-N receptor with the native *Drosophila* NRR (NRR^{Notch}) and FSHR-N with the LIN-12 NRR (NRR^{LIN-12}) are shown. Cleavage of the NRR^{Notch}-containing receptor is strictly Epsin dependent and does not respond to versions of FSH-Dl that are excluded from Epsin-dependent endocytosis, indicating a high force tuning. In contrast, the NRR^{LIN-12} receptor responds strongly to all three FSH-Dl ligands, indicating a lower force tuning. Representative images of these responses are shown on the right. $n = 4$ to 7 wing imaginal discs for each receptor-ligand pair. (**B** and **C**) Quantitation of the activation of FSHR-N variants by FSH-Dl, FSH-Dl-KtoR, or FSH-Dl-ΔIC. FSHR-N variants in which NRR^{Notch} was replaced with candidate domains from DCC, EphB2, DEph, Serrate, FAT1, Dscam1, VenusGFP, or DAG1, and representative images are shown. $n = 4$ to 23 wing imaginal discs for each receptor-ligand pair. Scale bars, 50 μm. Statistical comparisons of the average Cut distance/DV width ratios for each ligand-receptor pair were performed by Brown and Forsythe tests followed by Dunnett T3 post hoc analysis. $*P < 0.05$, $**P < 0.01$, $***P < 0.001$, and $****P < 0.0001$. WT, wild type.

B). This could be because there are few, if any, domain-intrinsic sequence and structural prerequisites for cleavage by ADAM10/Kuz or because the candidate switch domains are cleaved by other proteases. To resolve this uncertainty, we tested whether FSHR-Notch activity mediated by these domains depended on Kuz.

To do this, we used two permutations of MAPS technology, one for the ligand-dependent receptors and another for the constitutively active receptors. For both, we used the following RNA interference (RNAi)–mediated knockdown approach to greatly reduce Kuz activity in FSHR-Notch–expressing cells. Briefly, the expression of *UAS.Kuz-RNAi* under *nub.Gal4* control in otherwise wild-type wing discs renders Cut undetectable at the DV boundary, indicating strongly reduced Kuz activity. However, this knockdown can be rescued cell autonomously by coexpression of a *UAS.KuzHA* transgene, which is expressed in a sufficiently high amount to escape *UAS.Kuz-RNAi* knockdown of both endogenous *Kuz* and *UAS.KuzHA* transcripts (*37*). Hence, in animals that are otherwise wild type for the native *Kuz* gene, *UAS.KuzHA/UAS.Kuz-RNAi* transheterozygous cells are wild type for Kuz function and express hemagglutinin (HA)–tagged Kuz, whereas homozygous *UAS.Kuz-RNAi/UAS.Kuz-RNAi* cells do not express HA-tagged Kuz and have greatly diminished endogenous Kuz function. Thus, by generating transheterozygotes in which *UAS.Kuz-RNAi* is distal to *UAS>FSHR-Notch* on one chromosome and *UAS.KuzHA* is distal to *Ø>FSH-Dl* on the other, we were able to compare the ability of FSH-Dl–expressing cells to induce Cut expression in abutting FSHR-Notch–expressing cells depending on whether they retained or lacked Kuz activity (Fig. 5A; genetics described in detail in fig. S3).

We applied this test and found that all eight strictly ligand-dependent FSHR-Notch receptors and the benchmark receptors containing NRR^{Notch} and $NRR^{LIN\text{-}12}$ domains activated Cut expression in response to FSH-Dl from abutting signal-sending cells, but only if they retained Kuz function (Fig. 5B). Hence, ligand-dependent activation of all eight receptors and the two benchmark receptors depended on Kuz.

We also examined the Kuz requirement for activation of all three hyperactive receptors and a selection of six constitutively cleaved

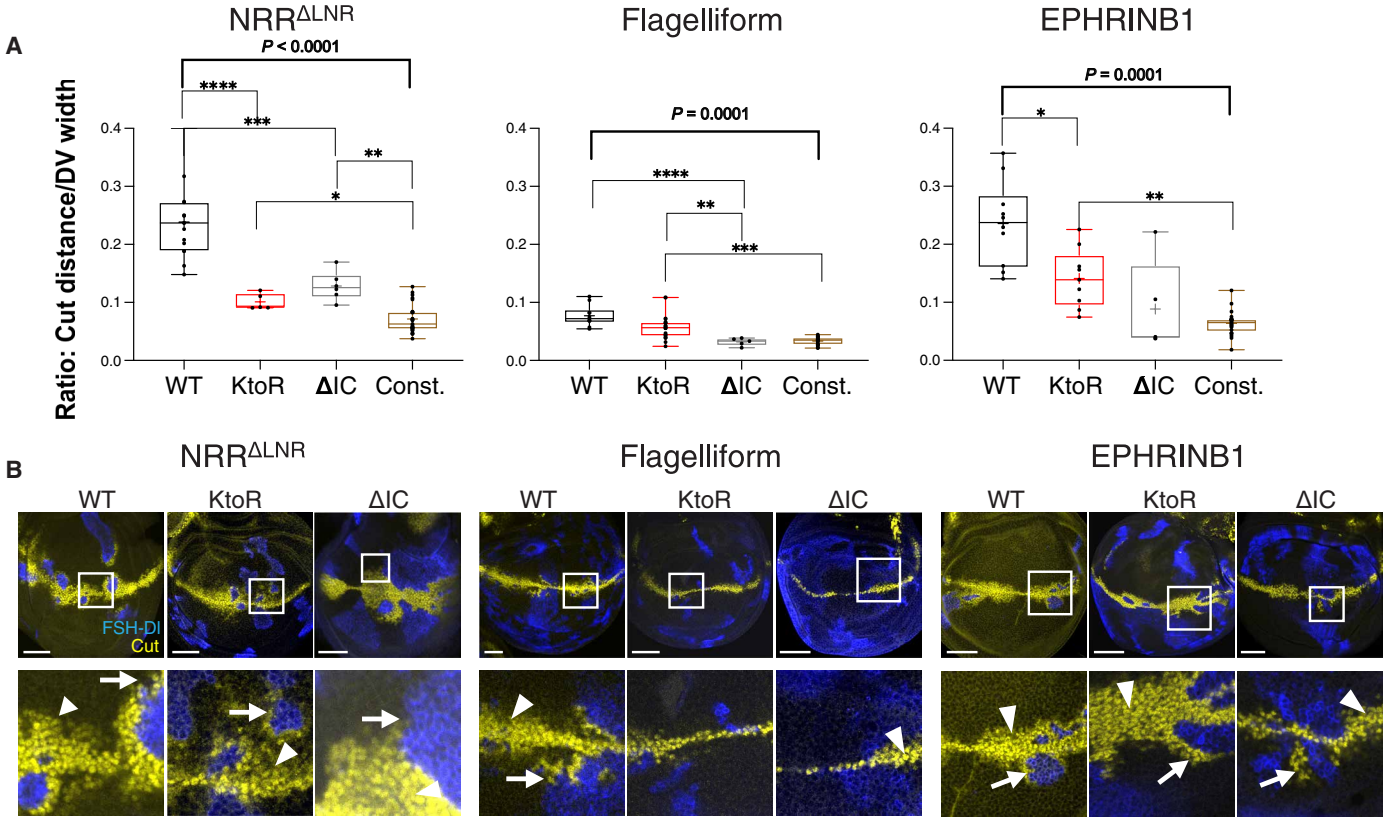

Fig. 4. Dependence of hyperactive receptors on Epsin-mediated ligand endocytosis. (**A**) Quantitation of the activation of FSHR-N hyperactive variants containing the candidate domains $NRR^{\Delta LNR}$, Flagelliform, or EPHRINB1 by FSH-Dl (WT), FSH-Dl-KtoR (KtoR), or FSH-Dl-ΔIC (ΔIC) and constitutive activation in the absence of ligand (Const). The distance ectopic Cut extended away from the DV boundary relative to disc size is presented as a ratio of the two distances. Signal strength is depicted as box plots that show the cut distance/DV width ratio for each disc as a point, as well as the mean (cross), median (horizontal line), and 25 to 75% interquartile ranges (tops and bottoms of the box) for each receptor-ligand combination. The amount of constitutive activation of each receptor was measured as the maximum distance of ectopic Cut from the DV boundary in regions of the wing away from clonal interfaces. Statistical comparisons of the average Cut distance/DV width ratios for each ligand-receptor pair were performed by Brown and Forsythe tests followed by Dunnett T3 post hoc analysis. $n = 4$ to 12 wing imaginal discs for each receptor-ligand pair; $^{*}P < 0.05$, $^{**}P < 0.01$, $^{***}P < 0.001$, and $^{****}P < 0.0001$. (**B**) Representative images showing Cut expression (yellow) in discs with clones expressing FSH-Dl, FSH-Dl-KtoR, or FSH-Dl-ΔIC (HRP^{+}, blue) and clones expressing the hyperactive FSHR-N receptors. Arrowheads indicate ectopic Cut detected in cells away from FSH-Dl–expressing cells. Arrows indicate areas furthest from the DV boundary where the receptor-expressing cells met ligand-expressing cells. Scale bars, 50 μm.

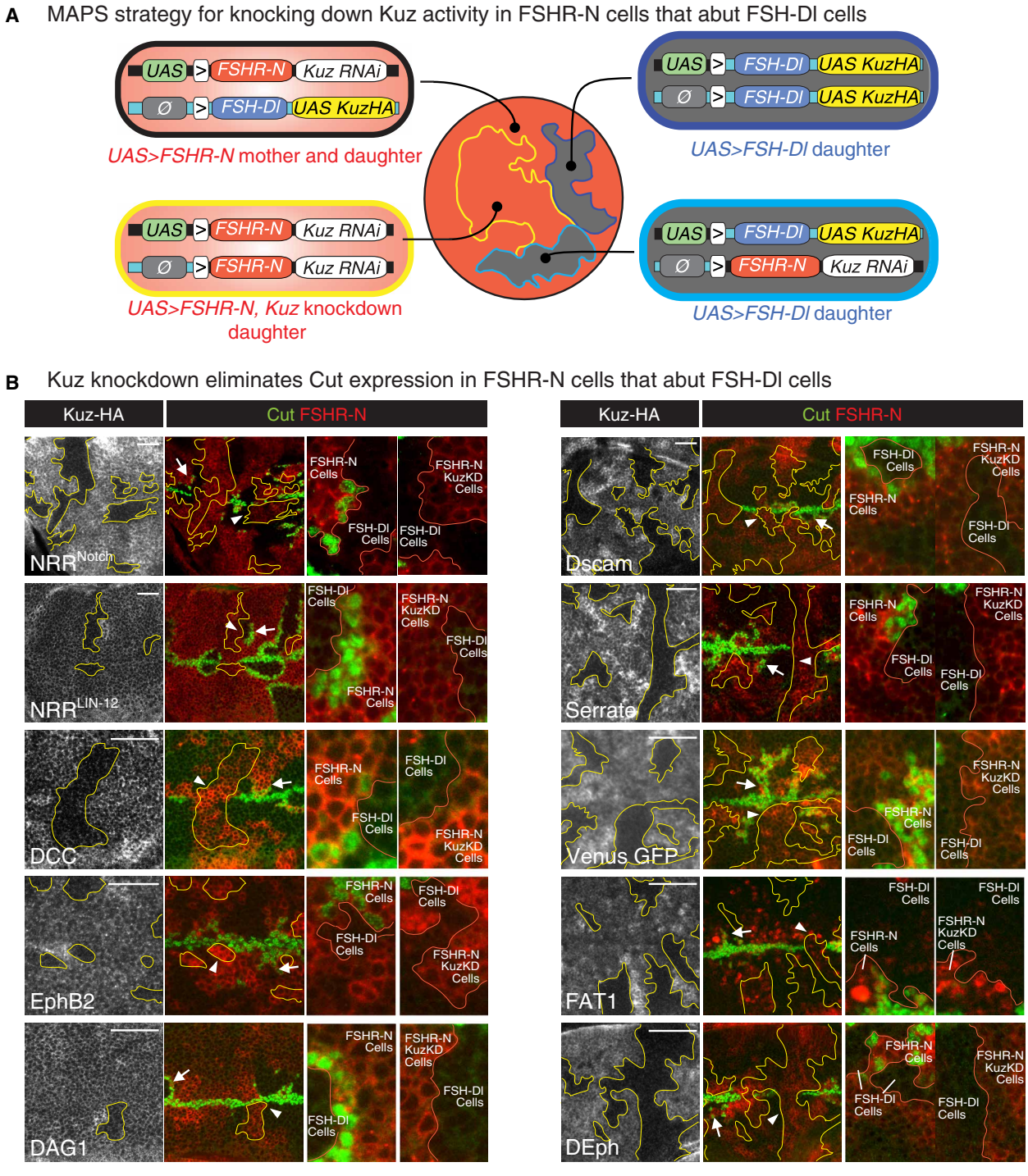

Fig. 5. The dependence on Kuzbanian for the cleavage of candidate proteolytic switch domains in response to Epsin-mediated ligand endocytosis. (**A**) MAPS technology used to knock down Kuz in genetically marked clones of FSHR-N–expressing cells. In transheterozygous mother cells, one chromosome carries *UAS>FSHR-N* with *UAS.Kuz-RNAi* (abbreviated as *Kuz RNAi* in the cartoon) positioned distally, and the other chromosome carries *Ø>FSH-DI* with *UAS.KuzHA* positioned distally. Cells of this genotype express FSHR-N but not FSH-DI and retain Kuz function. Mitotic recombination across the FRTs generates four kinds of daughter cells, depending on the two possible segregation events (fig. S3). Two of the four, outlined in blue, are "signal-sending" cells that express FSH-DI but not FSHR-N and retain Kuz function. The remaining two are "signal-receiving" cells that express FSHR-N but not FSH-DI, one of which is genetically identical to the mother cell and hence retains Kuz function (outlined in black), whereas the other is homozygous for *UAS.Kuz-RNAi* and subject to Kuz RNAi-mediated knockdown (outlined in yellow). (**B**) Staining for Cut (green) in wing discs with clones expressing FSHR-N receptors carrying the indicated candidate domains (Cherry$^+$, red) that either retain Kuz (HA$^+$, white) or have Kuz knocked down (HA$^-$, outlined in yellow). Signal-sending cells expressing FSH-DI are Cherry$^-$. Arrows indicate Cut in Kuz$^+$ receiving cells, and arrowheads indicate the absence of Cut in neighboring Kuz knockdown (KD) receiving cells (shown at higher magnification with the mosaic border indicated in red). Images are representative of $n = 3$ to 5 wing imaginal discs. Scale bars, 25 μm.

receptors (Fig. 6, A to D). For the three hyperactive receptors, the position of the receptor clone relative to the ligand clone was not crucial because each receptor showed modest activity in the absence of ligand. We therefore compared the activation of the receptors in the presence or absence of the *UAS.Kuz-RNAi* transgene using a "twin-spot" MAPS strategy that allowed us to assess both the weak constitutive and strong ligand-dependent responses in Kuz knockdown and control wing discs (Fig. 6A). For control discs expressing the ligand-dependent benchmark receptors (NRR^{Notch} or the $A2^{E1638K}$ switch domains), ectopic Cut was produced at mosaic borders at which one or both clonal cell populations were homozygous for either *UAS>FSHR-Notch* or *UAS>FSH-Dl*. In the Kuz knockdown discs, Cut was not induced along the DV boundary, and FSH-Dl/FSHR-Notch signaling did not induce ectopic Cut for either the NRR^{Notch} or $A2^{E1638K}$ receptors (Fig. 6B). For the hyperactive receptors carrying the Flagelliform, EPHRINB1, or $NRR^{\Delta LNR}$ candidate domains, control wing discs showed extensive Cut activation in most FSHR-Notch–expressing cells. The Kuz knockdown discs expressing the same receptors did not show Cut in *UAS>FSHR-Notch* cells, except for the Flagelliform-containing FSHR-Notch receptor, where residual Cut was detectable in homozygous *UAS>FSHR-Notch* clones that were positioned close to the DV border (Fig. 6B). Therefore, the benchmark receptors and all three hyperactive receptors behaved as Kuz dependent in this assay, as was also the case for control receptors carrying either NRR^{Notch} or the $A2^{E1638K}$ domains.

For six of the constitutively active receptors, we used a simpler, non-MAPS strategy in which FSH-Dl and FSHR-Notch were expressed in all cells of control or knockdown wing discs (Fig. 6C). For

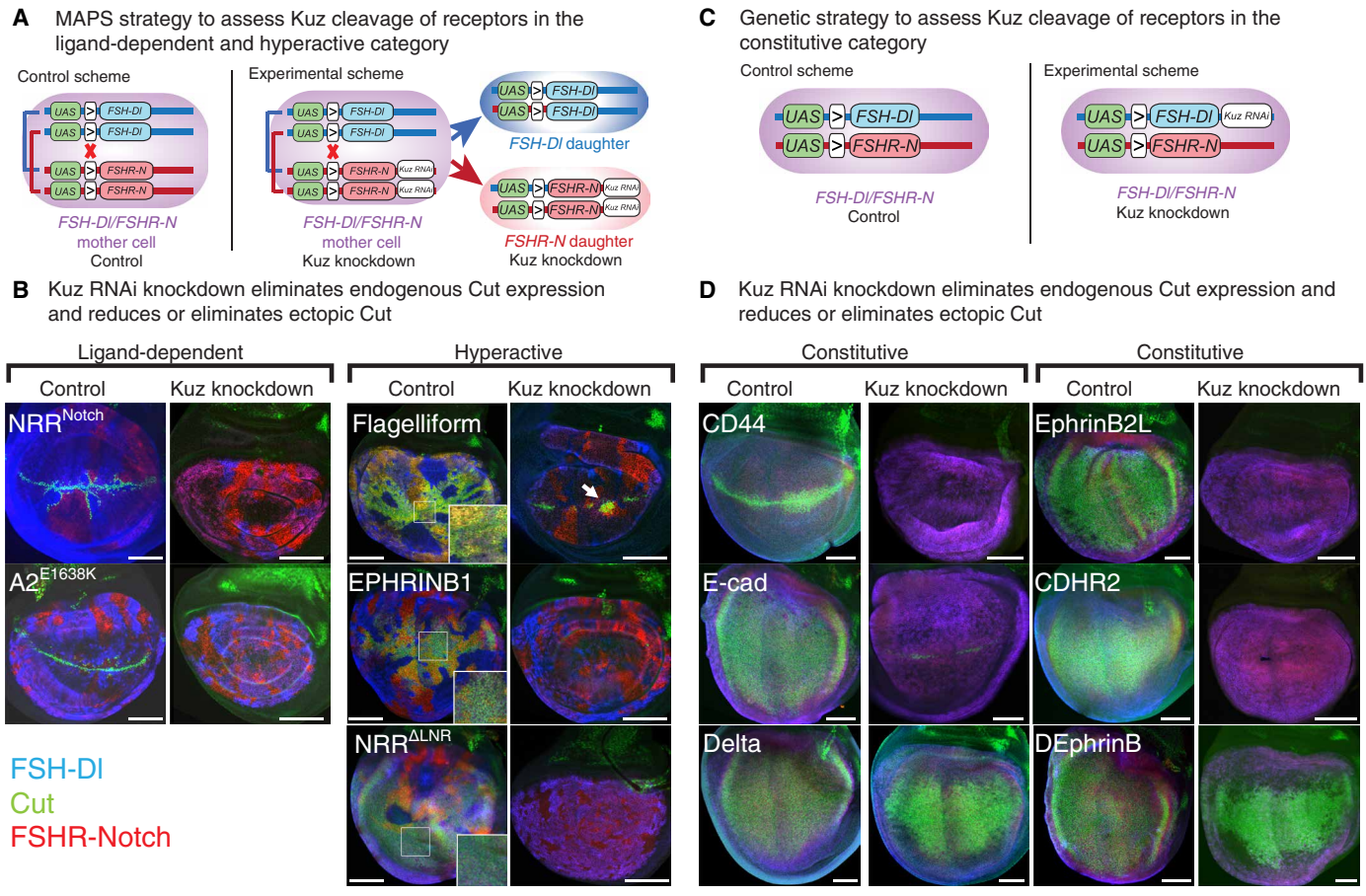

Fig. 6. FSHR-Notch receptors with hyperactive and constitutive activation require Kuzbanian. (**A**) MAPS strategy to assess Kuz cleavage of ligand-dependent and hypersensitive FSHR-N receptors. The control scheme uses the twin spot MAPS paradigm, with a *UAS>FSHR-N/UAS>FSH-Dl* parental cell and twin spot daughter cells homozygous for either *UAS>FSHR-N* or *UAS>FSH-Dl*. Note that in transheterozygous (mother) cells, canonical FSH-Dl and FSHR-N proteins bind in cis, precluding productive trans interactions. As a consequence, Cut activation is only induced at mosaic interfaces in which one or both clonal cell populations are homozygous for either *UAS>FSHR-N* or *UAS>FSH-Dl*. The experimental scheme generates FSH-Dl/FSHR-N interfaces in which Kuz is knocked down in all FSHR-N–expressing cells. This genotype is identical to the control scheme except for the addition of *UAS.Kuz-RNAi* distal to *UAS>FSHR-N*. (**B**) Staining for Cut (green) in wing discs containing clones of cells expressing FSH-Dl (HRP^+, blue) and clones of cells expressing hyperactive FSHR-N receptors containing the indicated candidate domains ($Cherry^+$, red) with or without Kuz knockdown after mitotic recombination as in (A). Receptors containing the NRR^{Notch} or $A2^{E1638K}$ switch domains are ligand-dependent benchmarks. Insets are higher magnification images of Cut expression in FSHR-N–expressing cells. The arrow indicates a clone of FSHR-N–expressing Kuz knockdown cells positioned close to the DV border in which Cut expression was retained. Images are representative of $n = 6$ to 10 wing imaginal discs. (**C**) Genetic strategy to assess Kuz cleavage of constitutive FSHR-N receptors. Both control and experimental schemes assess Cut in transheterozygous cells that are *UAS>FSHR-N/UAS>FSH-Dl*, with the experimental genotype also including *UAS.Kuz-RNAi* in cis with *UAS>FSH-Dl*. (**D**) Staining for Cut in control and Kuz-knockdown wing discs expressing both FSH-Dl (HRP^+, blue) and constitutively active FSHR-N receptors containing the indicated candidate domains ($Cherry^+$, red). Images are representative of $n = 6$ to 10 wing imaginal discs. Scale bars, 50 μm.

each of these constitutively active FSHR-Notch receptors, Cut was uniformly expressed throughout most or all of the wing pouch in the control, except for the more weakly constitutively active CD44 FSHR-Notch receptor, where Cut was ectopically expressed only in the vicinity of the DV border. In the Kuz knockdown discs, the Cut response was abolished in four of the six of these receptors, indicating that they behaved as strictly Kuz dependent. However, Cut was expressed in the Kuz knockdown discs for the remaining two of the six receptors with candidate domains from *Drosophila* Delta and EphrinB, suggesting that they are cleaved in a Kuz-independent manner (Fig. 6D). Hence, with two possible exceptions, the activation of all of the chimeric FSHR-Notch receptors tested, whether ligand dependent or constitutive, depended on the Kuz protease.

DISCUSSION

We present a readily scalable *Drosophila* screen to identify protein domains that can substitute for the NRR of Notch and activate the receptor in response to Epsin-mediated ligand endocytosis. In an initial, proof-of-principle test of 43 candidate domains, around one-quarter (11 of 43) had this capacity and comprised a diverse repertoire of seemingly unrelated structural motifs. Further, in every case, activation required Kuz, the sole *Drosophila* ADAM10 protease responsible for cleaving the NRR to activate native Notch. These results (i) validate the screen, (ii) provide insight into the structural basis and cleavage of force-sensitive proteolytic switches by ADAM10 proteases, (iii) provide the means to identify new proteolytic switches for synNotch biomedical applications, and (iv) raise the possibility that force-sensitive signaling mechanisms may be more prevalent than currently appreciated.

A scalable screen to identify protein domains that are cleaved in response to force

In our initial screen, we were able to quickly and unequivocally identify around half of the candidate proteolytic switches (23 of 43) as capable of mediating Notch activation when introduced in place of the native, force-dependent NRR domain. Of these, 11 of 23 exhibited ligand dependence, whether stringent (8 of 11) or more relaxed (3 of 11), whereas the remaining 12 of 23 conferred constitutive activity. We found that designations made on the basis of alterations in adult wing morphology following a simple genetic cross were validated by the analysis of Notch target gene expression in wing imaginal discs. Further, we were able to test and establish the requirements for Epsin-dependent ligand endocytosis and Kuz proteolysis for each of the 11 ligand-dependent proteolytic switches. Last, we optimized the methods used to conduct the screen, providing the potential to scale up the approach to assess hundreds rather than tens of different candidate proteolytic switches.

A large and diverse collection of sequences can behave as force-sensitive proteolytic switches

Our initial choice of candidate proteolytic switches was biased, in part, by prior evidence that other juxtacrine signaling systems aside from DSL-Notch might likewise depend on force-dependent cleavage mechanisms. These include Eph-Ephrin, Frazzled-DCC, and the Dscam family of proteins, all of which have roles in neuronal guidance (*38*). Some of these proteins share phenomenology with the Notch receptor, including γ-secretase cleavage following ADAM10 cleavage (*25*), transendocytosis of parts of the ligand-receptor bridge from one cell to another (*39*, *40*), and intracellular domains that may act as transcription factors (*37*, *41*). Other protein domains we tested were chosen on the basis of their structural or functional properties [from (*28*); Flagelliform] or serendipitous observations (Venus fluorescent protein). However, regardless of the justifications for choosing the candidates, the domains that tested positively for ligand-, Epsin-, and Kuz-dependent activation exhibit broad structural diversity as assessed by AlphaFold predictions.

That we observe such diversity among proteolytic switches suggests that the sequence and structural space for Kuz-dependent force sensing domains are large. Force-induced conformational changes in the Notch NRR appear to relieve steric hindrance of the target cleavage, possibly by removing a leucine "plug" that would otherwise occlude it (*17*, *31*, *42*). The new proteolytic switches we identified may function similarly, adopting conformation states in which specific structural elements must be displaced by force to expose one or more putative target sites for Kuz cleavage. In contrast, the constitutively cleaved domains presumably lack such steric hindrances, leaving their putative target sequences accessible to Kuz even in the absence of force. Alternatively, it is possible that the sole determinant of whether Kuz cleaves a given protein domain may be whether the target domain can be unfolded. Accordingly, all protein domains that adopt a folded conformation under normal physiological conditions would have the potential to substitute for the native Notch NRR if they can be unfolded by the ligand-dependent pulling force.

It may also be that factors other than simply exposure of the substrate cleavage site are important in the precise regulation of cleavage in different contexts. Possibilities include the action of tetraspanin proteins that place the protease active site at the substrate in a position poised for cleavage (*43*) and autoinhibitory structures within the protease that potentially have a capacity to respond to mechanical tension (*44*). Curiously, the ADAMTS13 protease that cleaves native VWF docks with the substrate, poised just above the occluded cleavage site to execute the cleavage if the site is rendered accessible by torsional strain (*45*). Hence, at least some of the specificity for Kuz/ADAM10 cleavage of the Notch NRR may similarly depend on the docking of the protease to the receptor, whether directly or through a bridging protein. Because the proteolytic switches we have identified all operate in the context of the FSH-Dl/FSHR-Notch signaling paradigm in which the receptor retains only the transmembrane and intracellular domains of native Notch, any such docking of Kuz would presumably have to be to these domains.

Three other aspects of our findings are worthy of note. First, the 11 candidate domains that tested positively for ligand, Epsin, and Kuz dependence appear to fall on a spectrum reflecting requirements for different amounts of Epsin-mediated endocytic force. Specifically, 5 of 11 were strictly dependent on Epsin-mediated ligand endocytosis, as determined by their failure to mediate Notch activation in response to modified forms of the ligand that have limited or no ability to enter the Epsin pathway. In contrast, three of the six of the remaining candidate domains activated Notch, albeit weakly, in response to these same modified ligands, a result we interpret as evidence that these domains are tuned to a lower force threshold. Last, the remaining three ligand-dependent domains appeared to confer both a heightened response to ligands that cannot enter the Epsin pathway and modest constitutive activity. Accordingly, we infer that they constitute a distinct class of hyperactive proteolytic switches tuned to an even lower amount of force.

Second, the hyperactive class includes a partially deleted form of the Notch NRR that retains little else except the defined Kuz cleavage site, consistent with the peptide sequence containing only the cleavage site retaining some residual capacity to function as a force-sensitive proteolytic switch. The hyperactive receptors also produced a response to ligand in cells located multiple cell diameters away from the ligand-presenting cells. We have recapitulated this phenomenon using simulations of the activation of especially potent receptors in which cell proliferation displaces responding cells away from ligand-expressing cells (*46*). Alternatively, a long-distance response to FSH-Dl could reflect heightened sensitivity to signaling mediated by filopodial extensions that can extend several cell diameters away from signal-sending and/or signal-receiving cells, as documented for native DSL-Notch signaling (*47*, *48*).

Third, the properties of all of the candidate switch domains contrast with properties of the native NRR from the *C. elegans* Notch protein LIN-12 (*31*). In this case, the receptor can be strongly activated by ligand whether or not it has access to the Epsin pathway but appears devoid of activity in the absence of ligand. We speculate that the $NRR^{LIN\text{-}12}$ composes a special kind of proteolytic switch that has been evolutionarily selected to respond nonlinearly to force, such that it can be strongly activated even in the absence of Epsin-mediated endocytosis while remaining strictly ligand dependent.

Prevalence of force-sensitive intercellular signaling mechanisms

A major motivation for screening for new NRR-like proteolytic switches is the conjecture that force-dependent Kuz cleavage may apply to other juxtacrine signaling interactions in addition to DSL/Notch signaling. Of particular interest, four of the ligand-dependent switches identified in the screen (Dscam1, DCC, EphB2, and DEph) function in contact-dependent signaling between neurons, a context in which there is evidence that piconewton forces can be generated across ligand-receptor intercellular bridges, whether by Epsin-mediated ligand endocytosis (*49*) or other means (*50*). A mechanosensitive cleavage mechanism in this context could have important functional consequences, such as the release of intracellular domains that act as transcription factors (*41*, *51*) or the transendocytosis of the bridge from one cell to another (*40*). Overall, the success of this screen in identifying a diverse repertoire of switches is consistent with mechanosensitive ADAM cleavage being a general principle of juxtacrine communication. One clear implication is that it will be difficult, if not impossible, to anticipate the presence of such a switch in any given signaling protein by its sequence or structural properties. Instead, identification will depend on functional tests.

The importance of functional testing is reinforced by the results we obtained with seven human candidate domains (table S1) previously tested for proteolytic switch behavior in cell culture (*28*). Two-thirds of the domains that scored positively in this cell culture assay also scored positively in our FSH-Dl/FSHR-Notch paradigm, but the remaining domain (from CDHR2) behaved constitutively. Similarly, three-fourths of the domains that scored negatively in cell culture did so in the fly wing, but the remaining domain (the E1638K mutant form of the VWF A2 domain) behaved as ligand dependent (*18*). The high, but incomplete, concordance between the two assays underscores the value of both assays in identifying robust switch domains.

Increasing the repertoire of proteolytic switches for synNotch biomedical applications

synNotch technologies using chimeric ligands and receptors to generate new, heterologous signaling systems offer potential for disease therapies and tissue engineering (*29*, *30*). The in vivo *Drosophila* screen presented here is both effective and scalable; therefore, it provides a new approach to identifying proteolytic switches that can be used to optimize and diversify the current repertoire of synNotch signaling systems, for example, to generate synNotch receptors with distinct force thresholds or signal-to-noise ratios. As such, it augments current approaches of synNotch development, for example, using truncations of the NRR and heterologous cleavage domains in the context of the SNIPR synNotch receptor (*52*). Last, the strategy of using model organisms to test synNotch components in vivo may help close the gap between the development of synNotch signaling systems and their clinical application (*53*).

MATERIALS AND METHODS

Drosophila

All flies were maintained at 25°C on standard corn food. Fly stocks were maintained at 18°C, whereas experiments were performed at 25°C.

Drosophila transgenes

All ligand and receptor coding sequences, with the exception of FSHα, were inserted into a modified form of *pUAST-attB* (www.flyc31.org, GenBank: EF362409.1) that contains a single Flp Recombinase Target (FRT, ">") positioned between the UAS promoter and the coding sequence, and the resulting *UAS>ligand* and *UAS>receptor* transgenes were introduced at a single genomic docking site, *attP-86Fb* located on the right arm of the third chromosome, oriented so that the promoter is centromere proximal to the coding sequence. Each transgene vector was "bar-coded" with one or two of several eye (w+, Rap rough eye phenotype), wing, bristle, or cuticle color (y+) marker genes that were used for identification following microinjection of mixtures of transgenes. A "no promoter" (Ø) element encoding the transcriptional terminating 3′ untranslated region of the *hsp70* gene is used in place of the UAS promoter in *Ø>ligand* transgenes [generated by Flp/FRT mitotic recombination in the male germline (*18*)]. A single *UAS.FSH*α transgene inserted by conventional P-element–mediated transformation onto the X chromosome was used in all experiments except negative controls, where it was omitted to prevent ligand/receptor binding.

The WT, KtoR, and ΔIC chimeric forms of FSH-Dl (Fig. 1A) are described in detail (*18*). The KtoR variant intracellular domain is identical to the wild-type FSH-Dl ligand intracellular domain (AQEKDD.....CGTPHM), except that all lysines following the transmembrane domain are replaced by arginine (AQERDD....CGTPHM). For all the ligands, the native extracellular domain of Dl was replaced in its entirety by the β subunit of human FSH (FSHβ) (*54*), and an HRP tag was inserted immediately downstream of the C-terminal YCSFGEMKE sequence of FSHβ and immediately upstream of the Dl transmembrane domain. FSHα was coexpressed with the FSHβ-Dl protein to reconstitute FSH, which is an FSHα/FSHβ heterodimer (for simplicity, we refer to all ligands as FSH-Dl chimeras and do not include the HRP tag in their designations).

The chimeric forms of Notch (Fig. 1, A and B) are based on the FSHR-Notch receptor described in detail (*18*). Briefly the N-terminal

epidermal growth factor (EGF) repeat containing portion of the native extracellular domain of Notch was replaced by the ectodomain of FSHR. The extracellular domain was tagged by the insertion of Cherry just upstream of the juxtamembrane NRR domain.

For the screen, the native NRR was replaced with the coding sequence of the candidate domain of interest. In each case, the same restriction enzyme sites (Avr II and Not 1) and junction sequences were used. The sequence of the NRR insertion position is between the upstream Cherry epitope tag and the downstream Notch transmembrane domain. For example, the junction sequences for the LIN-12 benchmark receptor were delykprNLTGF.....GNNTGFLrppanvkybit, delykprVLAPP.....ILSNLNGrppanvkybit for the Dscam1 candidate, and delykprAPSAV.....SIKEKLPrppanvkybit for the EphB2 candidate (the LIN-12 and candidate sequences in uppercase). The amino acid sequence of each of the ligand dependent and constitutive switch domains inserted at this position is given in table S3. Complete DNA sequences for both the ligands and receptors are available on request.

Drosophila genotypes

The genotypes used were as follows: *hsp70.flp* (BDSC Stk# 23649, Flybase ID: FBtp0001101), *nub.gal4* (BDSC Stk# 42699, Flybase ID: FBtp0009119), *UAS.Kuz-RNAi* (Flybase ID: FBal0179253) (*37*), *UAS.KuzHA* (BDSC Stk# 5816, Flybase ID: FBtp0007245), *y w hsp70.flp UAS.FSHα; nub.Gal4; Ø > FSHβ-Dl/SM6-TM6B*, (*18*), *y w hsp70.flp UAS.FSHα; nub.Gal4; Ø > FSHβ-Dl-KtoR/SM6-TM6B*, (*18*); *y w hsp70.flp UAS.FSHα; nub.Gal4; Ø > FSHβ-Dl-ΔIC/SM6-TM6B,* (*18*), *y w hsp70.flp; Sp/CyO; UAS > FSHR-NRR^{Notch}-Notch,* (*18*), *y w hsp70.flp; Sp/CyO; UAS > FSHR-NRR^{LIN-12}-Notch,* (*31*), *y w hsp70.flp; Sp/CyO; UAS > FSHR-CD-Notch,* (CD = candidate domain sequence; table S3), *y w hsp70.flp; Sp/CyO; UAS > FSHR-CD-Notch, UAS.KuzRNAi/TM6B,* and *y w hsp70.flp UAS.FSHα; nub.Gal4; Ø > FSH-Dl, UAS.KuzHA/SM6-TM6B.*

Analysis of signaling between dedicated ligand and receptor expressing cells

Signaling between dedicated ligand and receptor cells was analyzed using MAPS [see (*18*) for detailed description]. In essence, mitotic recombination across the FRTs in cells trans-heterozygous for *UAS>* and *Ø>*transgenes is induced in the presence of a *nub.Gal4* driver that acts in the developing wing. The appropriate segregation of the recombined chromatid arms at the four-strand stage generates mutually exclusive populations of ligand and receptor expressing cells; the ligand expressing cells are marked by staining for the HRP epitope tag (blue in all the figures), and the receptor expressing cells are marked "black" by the absence of ligand expression (and when needed, red, by the Cherry epitope tag on the receptor). Signaling is monitored by assaying for ectopic expression of Cut protein from the Notch target gene *cut* in receptor expressing cells that abut ligand expressing cells along the MAPS ligand/receptor mosaic interface.

To induce mosaics by promoter swap, first or second instar larvae of the appropriate genotype were heat shocked at 36°C for 1 hour, and wing discs from mature third instar larvae were dissected, fixed (2% formaldehyde and 0.1% Triton for 30 min; room temperature), washed three times in PBT [phosphate-buffered saline (PBS), 0.1% Triton, and 1% bovine serum albumin], and incubated in primary antibody in PBT. Commercially available mouse monoclonal anti-Cut (1:100; Mab Developmental Studies Hybridoma bank 2B10), and rabbit anti-HRP (1:1000; Abcam ab34885) or rabbit anti-HA (1:1000; Abcam ab236632) antisera were used, and incubation was carried out either at room temperature for 2 hours or overnight at 4°C. The tissue was then washed as before and incubated in PBT with secondary antibody (Alexa 488– and 633–conjugated labeled secondary antisera) before a final wash and mounting for confocal visualization [as in (*18*)]. The Cherry epitope tag was also readily visualized in these preparations, although only shown in Figs. 5 and 6 (both the HA and HRP epitopes require rabbit monoclonal antisera for detection, precluding our use of the anti-HRP antisera to mark the "ligand" clones in this context). The intensity of the Cherry signal was similar for all forms of the receptors analyzed, with any modest differences not correlating with their assignment into one of three distinct classes of response to ligand. Expression levels of the receptor were not further considered because we compared only relative levels of cleavage of the same receptor presented with different ligands. It is possible that receptors scored as refractory to cleavage were not strongly expressed.

Quantification and statistical analysis

In all *Drosophila* MAPS experiments, most if not all the imaginal wing discs contained several mutually exclusive subpopulations of ligand and receptor expressing cells within each wing primordium. For each FSHR-Notch variant, at least 10 progeny were examined from three independent crosses. In all cases, the results of each ligand/receptor combination are presented by representative images and quantitative analysis. As noted in the main text, Cut expression is normally induced in "border" cells flanking the DV compartment boundary in response to native DSL/Notch signaling, which peaks in the vicinity of the boundary and declines in a graded fashion as a function of distance from the boundary (*55*). Signaling between FSH-Dl and FSHR-Notch chimeras along MAPS mosaic borders located away from the DV boundary induces Cut when the combined inputs of the native and chimeric ligand/receptor interactions reach the levels normally required to induce Cut in DV border cells. Accordingly, the distances over which MAPS mosaic borders can induce Cut away from the boundary provide an indication of the strength of the signaling interaction between the chimeric ligand and receptor.

As depicted in Fig. 3A, we measured and averaged the maximum distances from the DV boundary over which ectopic Cut was detected along one to three MAPS mosaic borders in each of at least four and typically many more discs for each genotype (power analysis > 0.95, the numbers of discs analyzed for each ligand/receptor pair are presented in Figs. 3, A to C, and 4, A and B). Given that disc size varies, at least in part, because of extra growth induced by ectopic Notch activation, we normalized the average of the distances obtained in each disc by dividing it by the width of the DV compartment boundary within the prospective wing (the "Cut distance/DV width ratio"; Fig. 3A , *y* axis). Images were coded and measured by multiple individuals "blind" to the experimental genotype to eliminate bias.

Quantitation of the resulting ratios for each ligand/receptor pair are presented in Figs. 3 (A to C) and 4A in the form of box plots in which each point depicts the average of the ratios measured for a single disc, and the mean, median, and 25 to 75% interquartile ranges of the ratios are depicted by crosses, a wide horizontal line, and the tops and bottoms of each box, respectively. Statistical comparisons of the results obtained for different ligand/receptor pairs were performed by Brown and Forsythe tests followed by Dunnett T3 post hoc analysis using Graphpad software. Assessment of Cut expression

following Kuzbanian RNAi expression was replicated in at least three separate experiments for each receptor presented.

ColabFold structural predictions

For the AlphaFold computational analysis of protein structures (*56*), the open-source software ColabFold (*57*) was used (versions 1.3.0 and 1.5.2). The notebook "ColabFold: AlphaFold2 using MMseqs2" was used through the Google Collaboratory platform to run AlphaFold with the following parameters: use_templates = false, use_amber = true, msa_mode = "MMseqs2 (UniRef + Environmental)", model_type = "AlphaFold2-ptm", num_models = 5, model_order = [1, 2, 3, 4, 5], num_recycles = 6, rank_by = "plddt," max_msa = null, pair_mode = "unpaired + paired".

The amino acid sequences of the ligand-dependent domains of interest were entered to ColabFold for structure prediction using the specified parameters. No templates were used in the predictions. The AlphaFold algorithm generates five different structural models for each individual input. The models are ranked from best to worst based on the overall predicted Local Distance Difference Test (pLDDT), AlphaFold's per-residue confidence metric. Along with the structural models, the predicted aligned error of each model was visualized on a matrix. This metric implies a measure of confidence in the relative positions of residue pairs. The best confidence model prediction was chosen in each case and displayed in fig. S2.

Supplementary Materials

The PDF file includes:
Figs. S1 to S3
Tables S1 to S3

Other Supplementary Material for this manuscript includes the following:
MDAR Reproducibility Checklist

REFERENCES AND NOTES

1. R. A. Kovall, B. Gebelein, D. Sprinzak, R. Kopan, The canonical Notch signaling pathway: Structural and biochemical insights into shape, sugar, and force. *Dev. Cell* **41**, 228–241 (2017).
2. E. Gazave, P. Lapébie, G. S. Richards, F. Brunet, A. V. Ereskovsky, B. M. Degnan, C. Borchiellini, M. Vervoort, E. Renard, Origin and evolution of the Notch signalling pathway: An overview from eukaryotic genomes. *BMC Evol. Biol.* **9**, 249–227 (2009).
3. I. Greenwald, LIN-12/Notch signaling: Lessons from worms and flies. *Genes Dev.* **12**, 1751–1762 (1998).
4. T. Lieber, S. Kidd, M. W. Young, Kuzbanian-mediated cleavage of *Drosophila* Notch. *Genes Dev.* **16**, 209–221 (2002).
5. D. Pan, G. M. Rubin, Kuzbanian controls proteolytic processing of Notch and mediates lateral inhibition during *Drosophila* and vertebrate neurogenesis. *Cell* **90**, 271–280 (1997).
6. C. Brou, F. Logeat, N. Gupta, C. Bessia, O. LeBail, J. R. Doedens, A. Cumano, P. Roux, R. A. Black, A. Israel, A novel proteolytic cleavage involved in Notch signaling: The role of the disintegrin-metalloprotease TACE. *Mol. Cell* **5**, 207–216 (2000).
7. B. De Strooper, W. Annaert, P. Cupers, P. Saftig, K. Craessaerts, J. S. Mumm, E. H. Schroeter, V. Schrijvers, M. S. Wolfe, W. J. Ray, A. Goate, R. Kopan, A presenilin-1-dependent gamma-secretase-like protease mediates release of Notch intracellular domain. *Nature* **398**, 518–522 (1999).
8. G. Struhl, I. Greenwald, Presenilin is required for activity and nuclear access of Notch in *Drosophila*. *Nature* **398**, 522–525 (1999).
9. G. Struhl, A. Adachi, Requirements for presenilin-dependent cleavage of notch and other transmembrane proteins. *Mol. Cell* **6**, 625–636 (2000).
10. S. Kidd, T. Lieber, M. W. Young, Ligand-induced cleavage and regulation of nuclear entry of Notch in *Drosophila melanogaster* embryos. *Genes Dev.* **12**, 3728–3740 (1998).
11. M. Lecourtois, F. Schweisguth, Indirect evidence for Delta-dependent intracellular processing of Notch in *Drosophila* embryos. *Curr. Biol.* **8**, 771–775 (1998).
12. E. H. Schroeter, J. A. Kisslinger, R. Kopan, Notch-1 signalling requires ligand-induced proteolytic release of intracellular domain. *Nature* **393**, 382–386 (1998).
13. G. Struhl, A. Adachi, Nuclear access and action of Notch in vivo. *Cell* **93**, 649–660 (1998).
14. E. Overstreet, E. Fitch, J. A. Fischer, Fat facets and liquid facets promote Delta endocytosis and Delta signaling in the signaling cells. *Development* **131**, 5355–5366 (2004).
15. W. Wang, G. Struhl, *Drosophila* Epsin mediates a select endocytic pathway that DSL ligands must enter to activate Notch. *Development* **131**, 5367–5380 (2004).
16. W. Wang, G. Struhl, Distinct roles for Mind bomb, Neuralized and Epsin in mediating DSL endocytosis and signaling in *Drosophila*. *Development* **132**, 2883–2894 (2005).
17. W. R. Gordon, B. Zimmerman, L. He, L. J. Miles, J. Huang, K. Tiyanont, D. G. McArthur, J. C. Aster, N. Perrimon, J. J. Loparo, S. C. Blacklow, Mechanical allostery: Evidence for a force requirement in the proteolytic activation of Notch. *Dev. Cell* **33**, 729–736 (2015).
18. P. D. Langridge, G. Struhl, Epsin-dependent ligand endocytosis activates Notch by force. *Cell* **171**, 1383–1396.e12 (2017).
19. D. C. Sloas, J. C. Tran, A. M. Marzilli, J. T. Ngo, Tension-tuned receptors for synthetic mechanotransduction and intercellular force detection. *Nat. Biotechnol.* **41**, 1287–1295 (2023).
20. H. M. Tsai, I. I. Sussman, R. L. Nagel, Shear stress enhances the proteolysis of von Willebrand factor in normal plasma. *Blood* **83**, 2171–2179 (1994).
21. Q. Zhang, Y.-F. Zhou, C.-Z. Zhang, X. Zhang, C. Lu, T. A. Springer, Structural specializations of A2, a force-sensing domain in the ultralarge vascular protein von Willebrand factor. *Proc. Natl. Acad. Sci. U.S.A.* **106**, 9226–9231 (2009).
22. F. Tosetti, M. Alessio, A. Poggi, M. R. Zocchi, ADAM10 site-dependent biology: Keeping control of a pervasive protease. *Int. J. Mol. Sci.* **22**, 4969 (2021).
23. K. Hayashida, A. H. Bartlett, Y. Chen, P. W. Park, Molecular and cellular mechanisms of ectodomain shedding. *Anat. Rec. (Hoboken)* **293**, 925–937 (2010).
24. G. Weskamp, J. W. Ford, J. Sturgill, S. Martin, A. J. Docherty, S. Swendeman, N. Broadway, D. Hartmann, P. Saftig, S. Umland, A. Sehara-Fujisawa, R. A. Black, A. Ludwig, J. D. Becherer, D. H. Conrad, C. P. Blobel, ADAM10 is a principal 'sheddase' of the low-affinity immunoglobulin E receptor CD23. *Nat. Immunol.* **7**, 1293–1298 (2006).
25. P. W. Janes, N. Saha, W. A. Barton, M. V. Kolev, S. H. Wimmer-Kleikamp, E. Nievergall, C. P. Blobel, J.-P. Himanen, M. Lackmann, D. B. Nikolov, Adam meets Eph: An ADAM substrate recognition module acts as a molecular switch for ephrin cleavage in trans. *Cell* **123**, 291–304 (2005).
26. S. F. Lichtenthaler, M. K. Lemberg, R. Fluhrer, Proteolytic ectodomain shedding of membrane proteins in mammals-hardware, concepts, and recent developments. *EMBO J.* **37**, e99456 (2018).
27. C. I. Caescu, G. R. Jeschke, B. E. Turk, Active-site determinants of substrate recognition by the metalloproteinases TACE and ADAM10. *Biochem. J.* **424**, 79–88 (2009).
28. A. N. Hayward, E. J. Aird, W. R. Gordon, A toolkit for studying cell surface shedding of diverse transmembrane receptors. *eLife* **8**, e46983 (2019).
29. L. Morsut, K. T. Roybal, X. Xiong, R. M. Gordley, S. M. Coyle, M. Thomson, W. A. Lim, Engineering customized cell sensing and response behaviors using synthetic Notch receptors. *Cell* **164**, 780–791 (2016).
30. K. T. Roybal, L. J. Rupp, L. Morsut, W. J. Walker, K. A. McNally, J. S. Park, W. A. Lim, Precision tumor recognition by T cells with combinatorial antigen-sensing circuits. *Cell* **164**, 770–779 (2016).
31. P. D. Langridge, A. Garcia Diaz, J. Y. Chan, I. Greenwald, G. Struhl, Evolutionary plasticity in the requirement for force exerted by ligand endocytosis to activate *C. elegans* Notch proteins. *Curr. Biol.* **32**, 2263–2271 (2022).
32. F. J. Diaz-Benjumea, S. M. Cohen, Serrate signals through Notch to establish a Wingless-dependent organizer at the dorsal/ventral compartment boundary of the *Drosophila* wing. *Development* **121**, 4215–4225 (1995).
33. J. F. de Celis, A. Garcia-Bellido, S. J. Bray, Activation and function of Notch at the dorsal-ventral boundary of the wing imaginal disc. *Development* **122**, 359–369 (1996).
34. D. Doherty, G. Feger, S. Younger-Shepherd, L. Y. Jan, Y. N. Jan, Delta is a ventral to dorsal signal complementary to Serrate, another Notch ligand, in *Drosophila* wing formation. *Genes Dev.* **10**, 421–434 (1996).
35. N. Berndt, E. Seib, S. Kim, T. Troost, M. Lyga, J. Langenbach, S. Haensch, K. Kalodimou, C. Delidakis, T. Klein, Ubiquitylation-independent activation of Notch signalling by Delta. *eLife* **6**, 1752 (2017).
36. T. Troost, E. Seib, A. Airich, N. Vullings, A. Necakov, S. De Renzis, T. Klein, The meaning of ubiquitylation of the DSL ligand Delta for the development of *Drosophila*. *BMC Biol.* **21**, 260 (2023).
37. H. A. Coleman, J. P. Labrador, R. K. Chance, G. J. Bashaw, The Adam family metalloprotease Kuzbanian regulates the cleavage of the roundabout receptor to control axon repulsion at the midline. *Development* **137**, 2417–2426 (2010).
38. Y. Zang, K. Chaudhari, G. J. Bashaw, New insights into the molecular mechanisms of axon guidance receptor regulation and signaling. *Curr. Top. Dev. Biol.* **142**, 147–196 (2021).
39. A. C. Greene, S. J. Lord, A. Tian, C. Rhodes, H. Kai, J. T. Groves, Spatial organization of EphA2 at the cell-cell interface modulates trans-endocytosis of ephrinA1. *Biophys. J.* **106**, 2196–2205 (2014).
40. D. J. Marston, S. Dickinson, C. D. Nobes, Rac-dependent trans-endocytosis of ephrinBs regulates Eph-ephrin contact repulsion. *Nat. Cell Biol.* **5**, 879–888 (2003).

41. A. Neuhaus-Follini, G. J. Bashaw, The intracellular domain of the frazzled/DCC receptor is a transcription factor required for commissural axon guidance. *Neuron* **87**, 751–763 (2015).
42. W. R. Gordon, D. Vardar, G. Histen, C. Sanchez-Irizarry, J. C. Aster, S. C. Blacklow, Structural basis for the autoinhibition of Notch. *Nat. Struct. Mol. Biol.* **14**, 295–300 (2007).
43. C. H. Lipper, E. D. Egan, K. H. Gabriel, S. C. Blacklow, Structural basis for membrane-proximal proteolysis of substrates by ADAM10. *Cell* **186**, 3632–3641.e10 (2023).
44. T. C. M. Seegar, L. B. Killingsworth, N. Saha, P. A. Meyer, D. Patra, B. Zimmerman, P. W. Janes, E. Rubinstein, D. B. Nikolov, G. Skiniotis, A. C. Kruse, S. C. Blacklow, Structural basis for regulated proteolysis by the α-secretase ADAM10. *Cell* **171**, 1638–1648.e7 (2017).
45. J. T. Crawley, R. de Groot, Y. Xiang, B. M. Luken, D. A. Lane, Unraveling the scissile bond: How ADAMTS13 recognizes and cleaves von Willebrand factor. *Blood* **118**, 3212–3221 (2011).
46. J. E. Dawson, A. Bryant, B. Walton, S. Bhikot, S. Macon, A. Ajamu-Johnson, T. Jordan, P. D. Langridge, A. N. Malmi-Kakkada, Contact area and tissue growth dynamics shape synthetic juxtacrine signaling patterns. *Biophys. J.* **124**, 93–106 (2025).
47. M. Cohen, M. Georgiou, N. L. Stevenson, M. Miodownik, B. Baum, Dynamic filopodia transmit intermittent Delta-Notch signaling to drive pattern refinement during lateral inhibition. *Dev. Cell* **19**, 78–89 (2010).
48. C. De Joussineau, J. Soule, M. Martin, C. Anguille, P. Montcourrier, D. Alexandre, Delta-promoted filopodia mediate long-range lateral inhibition in *Drosophila*. *Nature* **426**, 555–559 (2003).
49. S. Kidd, G. Struhl, T. Lieber, Notch is required in adult *Drosophila* sensory neurons for morphological and functional plasticity of the olfactory circuit. *PLOS Genet.* **11**, e1005244 (2015).
50. D. Koch, W. J. Rosoff, J. Jiang, H. M. Geller, J. S. Urbach, Strength in the periphery: Growth cone biomechanics and substrate rigidity response in peripheral and central nervous system neurons. *Biophys. J.* **102**, 452–460 (2012).
51. S. M. Sachse, S. Lievens, L. F. Ribeiro, D. Dascenco, D. Masschaele, K. Horre, A. Misbaer, N. Vanderroost, A. S. De Smet, E. Salta, M. L. Erfurth, Y. Kise, S. Nebel, W. Van Delm, S. Plaisance, J. Tavernier, B. De Strooper, J. De Wit, D. Schmucker, Nuclear import of the DSCAM-cytoplasmic domain drives signaling capable of inhibiting synapse formation. *EMBO J.* **38**, e99669 (2019).
52. I. Zhu, R. Liu, J. M. Garcia, A. Hyrenius-Wittsten, D. I. Piraner, J. Alavi, D. V. Israni, B. Liu, A. S. Khalil, K. T. Roybal, Modular design of synthetic receptors for programmed gene regulation in cell therapies. *Cell* **185**, 1431–1443.e16 (2022).
53. S. M. Brooks, H. S. Alper, Applications, challenges, and needs for employing synthetic biology beyond the lab. *Nat. Commun.* **12**, 1390 (2021).
54. Q. R. Fan, W. A. Hendrickson, Structure of human follicle-stimulating hormone in complex with its receptor. *Nature* **433**, 269–277 (2005).
55. S. S. Blair, Limb development: marginal fringe benefits. *Curr. Biol.* **7**, R686–R690 (1997).
56. J. Jumper, D. Hassabis, Protein structure predictions to atomic accuracy with AlphaFold. *Nat. Methods* **19**, 11–12 (2022).
57. R. Nussinov, M. Zhang, Y. Liu, H. Jang, AlphaFold, artificial intelligence (AI), and allostery. *J. Phys. Chem.* **126**, 6372–6383 (2022).

Acknowledgments: We thank D. Huntley, O. Mosley, A. Bryant, N. Pampatwar, D. Dang, and C. Andrews for technical assistance. **Funding:** Research reported in this publication was supported by the National Institutes of Health through the Institute of General Medicine of the under award number R35 GM127141 (to G.S.) and the Institute of Child Health and Human Development under award number R21 HD107414 (to P.D.L.), in addition to support from the Roy and Diana Vagelos Precision Medicine Award (to G.S. and P.D.L.) and the Research Scholarship & Creativity Activity Program at Augusta University (to P.D.L.). The content is solely the responsibility of the authors and does not necessarily represent the official views of the National Institutes of Health. **Author Contributions:** Conceptualization: P.D.L. and G.S. Investigation: P.D.L., F.C.B., J.H., T.J., B.W., A.A.-J., R.F.A., and S.B. Writing—original draft: P.D.L. and F.C.B. Writing—review and editing: P.D.L., F.C.B., and G.S. Supervision: P.D.L. Funding acquisition: G.S. and P.D.L. **Competing interests:** The authors declare that they have no competing interests. **Data and materials availability:** All data needed to evaluate the conclusions in the paper are present in the paper or the Supplementary Materials. Further information and requests for resources and reagents should be directed to and will be fulfilled by P.D.L. (plangridge@augusta.edu).

Submitted 27 September 2024
Resubmitted 25 January 2025
Accepted 16 May 2025
Published 10 June 2025
10.1126/scisignal.adt4606